Available online at www.sciencedirect.com
SCIENCE DIRECT®
C. R. Mecanique 334 (2006) 98–104
COMPTES RENDUS MECANIQUE
http://france.elsevier.com/direct/CRAS2B/

Noise reduction of a Mach 0.7–0.9 jet by impinging microjets

Thomas Castelain [a,*], Jean-Christophe Béra [b,a], Michel Sunyach [a]

[a] *Centre acoustique, 36, avenue Guy-de-Collongue, 69134 Ecully, France*
[b] *INSERM U556, 151, cours Albert-Thomas, 69424 Lyon cedex 03, France*

Received 10 December 2005; accepted 10 January 2006

Presented by Geneviève Comte-Bellot

Abstract

A global noise reduction of a high-subsonic jet is achieved by experimental use of an impinging microjets system. The microjet velocity relative to the main jet velocity, the longitudinal distance of injection and the number of microjets are the three parameters examined in order to obtain the maximum noise reduction. This optimized microjet configuration is obtained by a balance between low-frequency attenuation and high-frequency noise generation due to the interaction between the microjets and the main jet mixing layer. ***To cite this article: T. Castelain et al., C. R. Mecanique 334 (2006).***

Résumé

Réduction du bruit d'un jet de Mach 0,7–0,9 par un système de microjets impactants. Cette étude concerne la réduction du bruit global d'un jet subsonique par un système de microjets impactants. Le rapport entre la vitesse des microjets et celle du jet principal, la distance longitudinale d'injection et le nombre de microjets sont les trois paramètres présentement étudiés pour atteindre un maximum de réduction de bruit. La configuration dite optimale correspond à un équilibre entre la réduction de bruit en basse fréquence et une régénération de bruit en haute fréquence due à l'interaction entre les microjets et la couche de mélange du jet principal. ***Pour citer cet article : T. Castelain et al., C. R. Mecanique 334 (2006).***

Keywords: Fluid mechanics; Jet; Noise reduction; Microjet

Mots-clés : Mécanique des fluides ; Jet ; Réduction de bruit ; Microjet

Version française abrégée

Les différents dispositifs, chevrons, dentelures ou tabs, qui ont déjà été développés pour réduire le bruit des jets [2–5] induisent en général une perte de poussée incompatible avec les contraintes de l'industrie aéronautique. Ils sont de surcroît difficilement amovibles. Un système de microjets tel que proposé dans ce travail a l'avantage de pouvoir être actionné uniquement pendant les phases critiques du vol, en dehors desquelles il n'induit pas de perte de poussée.

* Corresponding author.
E-mail address: thomas.castelain@ec-lyon.fr (T. Castelain).
URL: http://acoustique.ec-lyon.fr.

1631-0721/$ – see front matter
doi:10.1016/j.crme.2006.01.001

Il semble donc crucial de déterminer les paramètres géométriques et aérauliques d'un tel système maximisant la réduction de bruit.

Les essais réalisés en soufflerie anéchoïque ont porté sur un jet haut-subsonique ($M_j = 0{,}7$ et $M_j = 0{,}9$) contrôlé par un système de microjets dont la géométrie est décrite en Fig. 1. Trois paramètres du système de microjets ont été étudiés : la distance d'injection, la vitesse d'injection et le nombre de microjets.

L'effet de la distance longitudinale d'injection d, distance entre le point d'impact et la buse, est traduit sur la Fig. 2. La réduction du bruit global est plus élevée aux petites valeurs de d, quelle que soit la vitesse des microjets.

L'effet de la vitesse d'injection est étudié par une approche spectrale, avec une pondération de la Densité Spectrale de Puissance (PSD) par la fréquence f (Fig. 3). L'examen de ces spectres en Fig. 4 indique que la réduction du bruit en hautes fréquences, pour les fréquences de l'ordre de f_{co}, est d'autant plus faible que la vitesse est élevée, ce qui traduit l'existence d'un bruit d'interaction entre les microjets et la couche de mélange du jet principal. Parallèlement, la réduction de bruit aux fréquences contenant le maximum d'énergie, i.e., vers f_{peak}, augmente avec la vitesse des microjets. Si f_{peak} est suffisamment distinct de f_{co}, comme dans le cas $\theta = 30°$, le niveau de bruit global est uniquement déterminé par la réduction apportée aux fréquences proches de f_{peak}. Si f_{peak} et f_{co} sont proches, comme pour $\theta = 90°$, l'augmentation de la vitesse des microjets implique un gain de réduction vers f_{peak} compensé par la diminution de la réduction vers f_{co}.

L'effet du nombre de microjets utilisés permet de quantifier la réduction du bruit en terme du rapport r_m entre le débit total injecté pour le contrôle et le débit du jet principal (Fig. 5). On note l'efficacité des petites valeurs de r_m, de l'ordre de 3×10^{-3}, ce qui est un avantage par rapport à l'injection d'eau [12]. De plus pour un débit total de contrôle donné, la meilleure configuration correspond à celle qui implique le plus grand nombre de microjets. On note également que la réduction du bruit est une fonction linéaire du nombre de microjets employés, pour une vitesse d'injection fixée.

En conclusion, une configuration optimale du système de contrôle étudié permet une réduction de 2 dB du bruit global. Les mécanismes d'action des microjets sur le bruit de jet sont actuellement analysés, notamment par une analyse par Vélocimétrie par Images de Particules du champ aérodynamique du jet.

1. Introduction

Noise generation from high-speed turbulent jets remains a significant research topic, due to its crucial implication in the aeronautical industry. Despite experiments and numerical simulations on jets carried out over the last few decades, the fundamental mechanisms underlying jet noise have still to be determined. For supersonic jets, the feed-back loop mechanisms in noise generation have satisfactorily been described [1] and a good agreement between theory and experiments has been obtained for pure tone noise. The comprehension of the jet mixing noise, occurring both in supersonic and high-subsonic jets, still remains a challenge. Consequently, any jet control system able to modify—or to reduce—the emitted noise could make a significant advance.

Some passive systems, called teeth extensions [2], tabs or chevrons [3–5] have been suggested, but they can affect airplane performances due to thrust reduction. As an alternative, a micro-injection system impacting the main jet has also been suggested [6,8]. As in the passive devices mentioned above, such a system reduces the turbulence level in the entire mixing region of jets, and subsequently the noise radiated by the jet. The geometrical and aerodynamical parameters of the microjets system have, however, not been fully investigated. The present Note reports experiments on a system optimized for maximum noise reduction.

2. Experimental set-up

Experiments have been made in the supersonic anechoic facility of the Centre Acoustique, LMFA – École centrale de Lyon. The jet has a diameter D of 50 mm and is powered by a screw compressor of 450 kW with a maximum mass-flux of 1.7 $\mathrm{kg\,s^{-1}}$. After compression, the air was heated by a set of resistances of total power 80 kW, to set the temperature of the jet after the expansion to room temperature. The results presented in Sections 3 and 4 concern a jet Mach number based on the external speed of sound c_0 of $M_j = U_j/c_0 = 0.7$, the results of Section 5 a jet at $M_j = 0.9$.

The control system is made of up to 18 microjets directed toward the jet centerline and impacting the jet at an angle of 70° (see Fig. 1). The microjets are issued from straight brass tubes of 1 mm exit diameter, regularly set around

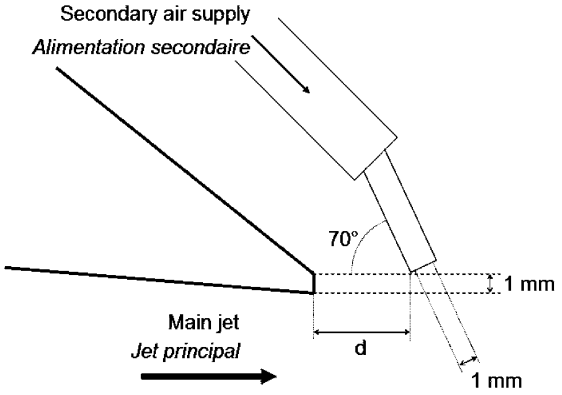

Fig. 1. Sketch of one microjet in the injection system.

Fig. 1. Schéma d'un microjet du système d'injection.

the circumference of the jet. The microjets are fed by a piston compressor, connected to a stage of micro-filters and a stage of two relief valves. Three parameters have been considered:

- the longitudinal distance d between the jet exit and the microjets system (see Fig. 1), the radial distance and the impact angle being kept constant;
- the microjet exit velocity, controlled by the low-pressure relief valve of the installation. This velocity is normalized by the main jet velocity, giving the parameter of interest $r = U_{\text{microjet}}/U_j$;
- the number of microjets, from 3 to 18.

The noise spectra are obtained with a B&K 4192 $1/2''$ microphone and a B&K 2804 Power Supply, connected to a HP 35652B acquisition module set in a Paragon spectrum analyser. The overall sound pressure levels (SPL) are computed by integrating the spectra from $f_1 = 200$ Hz to $f_2 = 22$ kHz, with a reference pressure $p_{\text{ref}} = 2 \times 10^{-5}$ Pa. The microphone is located at $40D$ from the jet exit centre, and θ is the angle between the downstream jet axis and the microphone.

The maximum difference between the acoustical measurements concerning a same configuration at different times of the acquisition procedure is below 0.1 dB SPL.

3. Effect of the longitudinal distance *d*

In this section the number of microjets is set to 18. Noise spectra were acquired for four longitudinal displacements of the control system, from $d \simeq 0$ to $d = 0.3D$. The SPL reduction at two angles θ is presented on Figs. 2(a) and 2(b). For each figure, the three curves correspond to three different values of the microjet velocity.

We first observe that a reduction in the jet noise is obtained whatever the values of d and of the injection velocity. Moreover, for a constant injection velocity, the noise reduction decreases as d increases. This result can be explained by the larger sensitivity of the initial mixing layer to perturbations at the jet exit, hence the energy needed to introduce aerodynamical modifications is lower at that location. Similar conclusions were obtained by [9] in the case of an acoustical excitation of a jet, applied at the jet exit.

The magnitude of the jet noise reduction is larger for $\theta = 90°$ (Fig. 2(b)) than at $\theta = 30°$ (Fig. 2(a)), for the entire range of distances d tested. The examination of the noise spectra (not represented) shows that the variation of noise attenuation with d is approximately uniform in frequency. As the noise radiated in the $\theta = 90°$ direction mainly comes from the mixing layer, and the noise in the $\theta = 30°$ direction is dominated by the directional noise sources located at the end of the potential core [10], the spectrum dynamic range is larger at 30° than at 90°. As a result, this observed frequency-uniform shift of the spectrum magnitude has a greater effect on the SPL at 90° than at 30°. Hence, whatever the injection velocity, the noise reduction in the $\theta = 90°$ direction is marginally more sensitive to d than that in the $\theta = 30°$ direction.

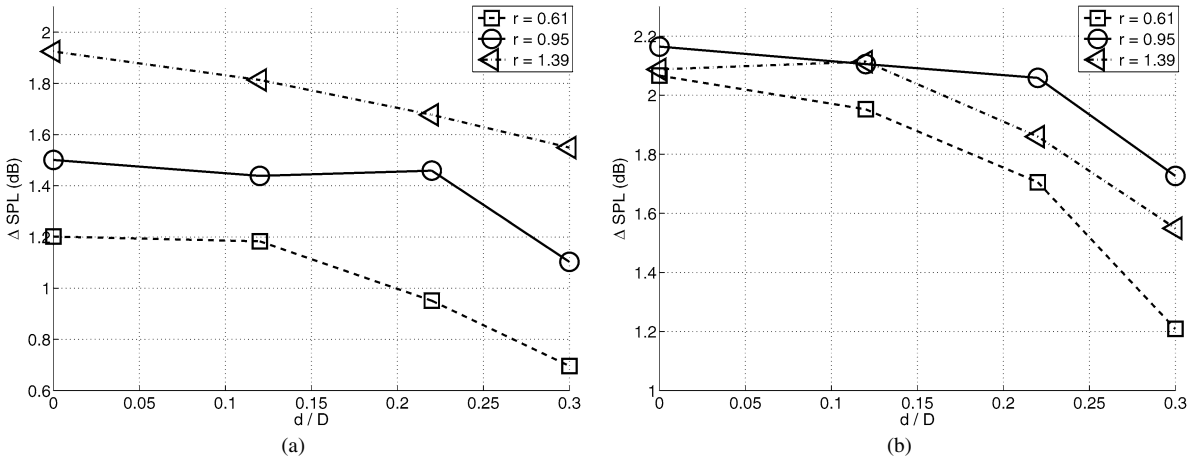

Fig. 2. Jet noise reduction (dB) with the longitudinal distance d of injection. Each of the three curves corresponds to a given velocity ratio; □: 0.61, ◯: 0.95 and ◁: 1.39. $M_j = 0.7$. (a) SPL reduction for $\theta = 30°$. (b) SPL reduction for $\theta = 90°$.

Fig. 2. Réduction du bruit de jet (dB) en fonction de la distance longitudinale d'injection d. Chacune des trois courbes correspond à une valeur du rapport des vitesses r ; □ : 0,61, ◯ : 0,95 and ◁ : 1,39. $M_j = 0{,}7$. (a) Réduction du niveau de bruit pour $\theta = 30°$. (b) Réduction du niveau de bruit pour $\theta = 90°$.

4. Effect of the microjet exit velocity

For this investigation, the number of microjets was set to 18, and the distance d was set to zero. The value of $d = 0$ permits the largest noise reduction as shown in Fig. 2. However, the noise reduction at $\theta = 30°$ is observed to be a monotonic function of the velocity ratio r, for all d. At $\theta = 90°$, the trend is not so clear: considering $d = 0.3D$, we observe that the highest velocity ratio does not match the highest noise reduction. The observation of the SPL levels alone is not sufficient to explain that trend, and the spectra have to be examined. Fig. 3(a) shows the Power Spectral Density (*PSD*) of the acoustical pressure $S(f)$ for $\theta = 30°$, the x-axis representing frequency and the y-axis being in $\mathrm{Pa}^2\,\mathrm{Hz}^{-1}$. The maximum of PSD occurs at $f_p = 950$ Hz, corresponding to a Helmholtz number $H_D = f_p D(1 - 0.5M_j\cos(\theta))/c_0 = 0.1$, in good agreement with other experiments [11].

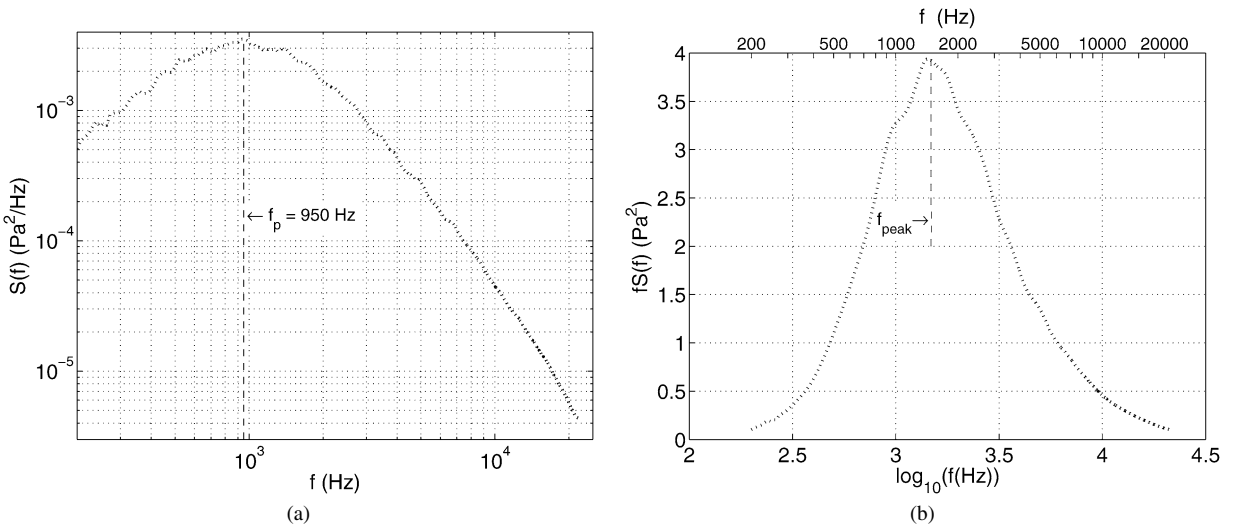

Fig. 3. Noise spectrum for the reference jet, with $\theta = 30°$ and $M_j = 0.7$. Left, Power Spectrum Density $S(f)$. Right, frequency-weighted spectra $fS(f)$. (a) $S(f)$ ($\theta = 30°$). (b) $fS(f)$ ($\theta = 30°$).

Fig. 3. Spectre du bruit de jet de référence, pour $\theta = 90°$ et $M_j = 0,7$. A gauche, Densité Spectrale de Puissance $S(f)$. A droite, spectre pondéré par la fréquence $fS(f)$. (a) $S(f)$ ($\theta = 30°$). (b) $fS(f)$ ($\theta = 30°$).

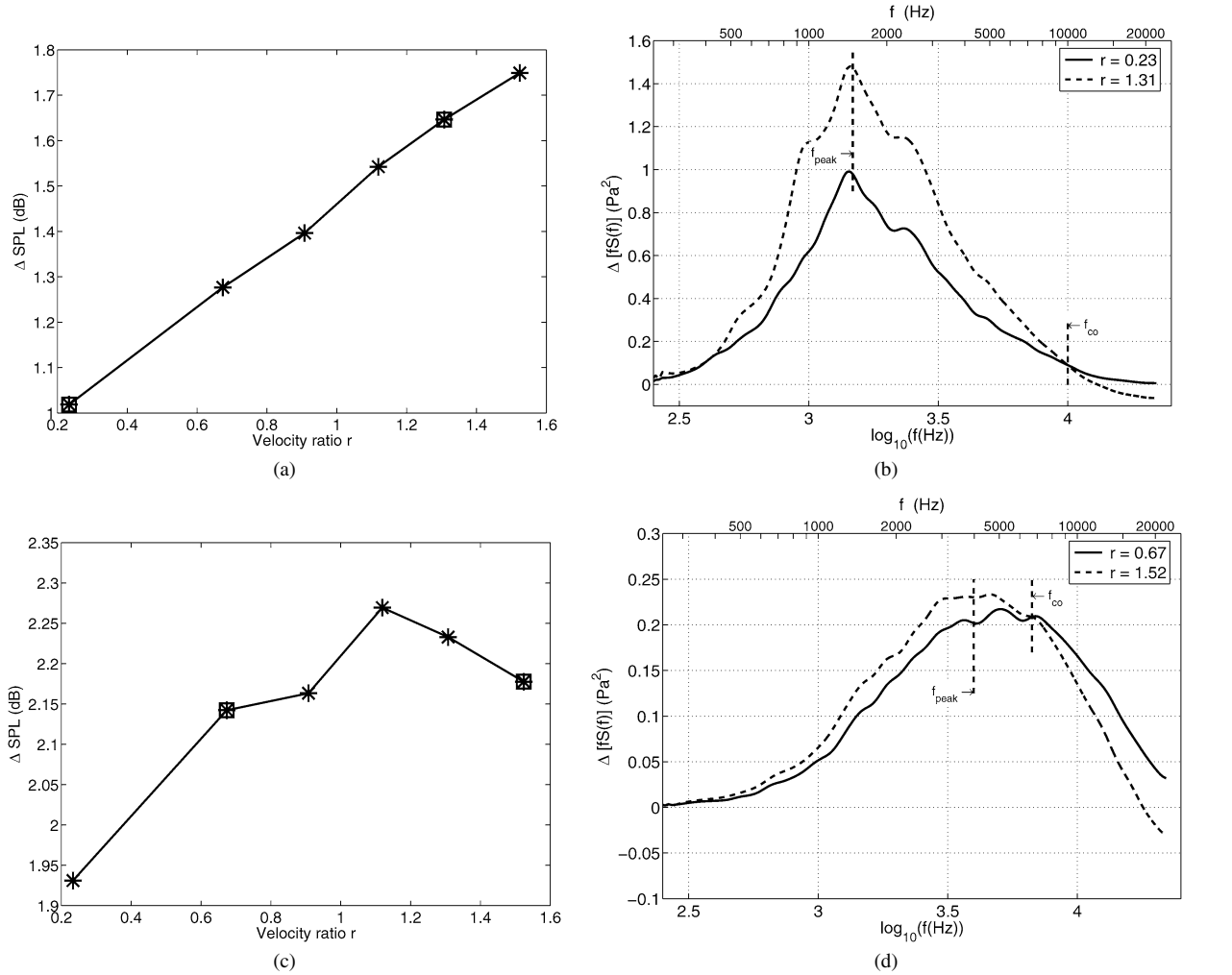

Fig. 4. Jet noise reduction for different microjet velocity ratios $r = U_{\text{microjet}}/U_j$. Left, SPL reduction: the square symbols correspond to the cases related in the spectra; right, differences between the spectrum for the reference jet noise ($r = 0$), and the two controlled cases with $r = 0.23$ and $r = 1.31$ for $\theta = 30°$, $r = 0.67$ and $r = 1.52$ for $\theta = 90°$. $d = 0$ and $M_j = 0.7$. (a) ΔSPL ($\theta = 30°$). (b) $\Delta[fS(f)]$ ($\theta = 30°$). (c) ΔSPL ($\theta = 90°$). (d) $\Delta[fS(f)]$ ($\theta = 90°$).

Fig. 4. Réduction du bruit de jet pour différentes valeurs du rapport des vitesses $r = U_{\text{microjet}}/U_j$. A gauche, réduction du niveau global : les symboles carrés correspondent aux valeurs de r dont on représente les spectres acoustiques. A droite, écarts entre le spectre acoustique du jet naturel ($r = 0$) et des deux cas de contrôle avec $r = 0{,}23$ et $r = 1{,}31$ pour $\theta = 30°$, et $r = 0{,}67$ et $r = 1{,}52$ pour $\theta = 90°$. $d = 0$ and $M_j = 0{,}7$. (a) ΔSPL ($\theta = 30°$). (b) $\Delta[fS(f)]$ ($\theta = 30°$). (c) ΔSPL ($\theta = 90°$). (d) $\Delta[fS(f)]$ ($\theta = 30°$).

Fig. 3(b) is a plot of the frequency weighted spectra $fS(f)$ versus $\log_{10}(f)$. With this linear and dimensionless x-axis, the y-axis in Pa^2 hence allows a direct estimate of the sound pressure level given by Eq. (1):

$$\text{SPL} = 10\log_{10}\frac{2.3\int_{\log_{10}(f_1)}^{\log_{10}(f_2)} fS(f)d(\log_{10}(f))}{p_{\text{ref}}^2} \tag{1}$$

In practice, $fS(f)$ is similar to the third-octave and octave spectra used in noise regulation laws [7].

Figs. 4(a) and 4(c) gives, for $\theta = 30°$ and $\theta = 90°$ respectively, the SPL reduction for the six values of r tested. Similarly, Figs. 4(b) and 4(d) compares the differences $\Delta[fS(f)]$ between the reference jet noise spectrum and the spectra corresponding to two significant values of r, i.e., $\Delta[fS(f)] = [fS(f)]_{\text{reference jet}} - [fS(f)]_{\text{controlled case}}$.

The noise reduction ΔSPL in the $\theta = 30°$ direction, given in Fig. 4(a), increases continuously with the microjet velocity, over the range of r tested. Fig. 4(b) provides the spectrum analysis of the noise reduction obtained for

$r = 0.23$ and $r = 1.31$. The largest reduction in the low-frequency range, around $f_{\text{peak}} = 1500$ Hz, is obtained for the highest value of r. This results in a higher SPL reduction, as the energy of the noise spectrum is mainly contained by this low-frequency range (see Fig. 3(b)). We also notice a cross over of the spectrum differences at $f_{\text{co}} = 10$ kHz, linked with a noise increase for $f > 12\,600$ Hz in the case of high value of r, which illustrates the modification of the high frequency jet noise sources.

In the $\theta = 90°$ direction, the noise reduction reaches a maximum for the velocity ratio $r = 1.1$, as illustrated in Fig. 4(c). Fig. 4(d) clearly shows similar results to those of Fig. 4(b), i.e., the higher r, the higher noise reduction of the most energetic frequency-range, which is centered on $f_{\text{peak}} = 4000$ Hz. Furthermore, the high frequency noise increase now affects the SPL reduction because f_{co} and f_{peak} are closed to each-other, i.e., $f_{\text{co}}/f_{\text{peak}} \simeq 1.75$, whereas in the $\theta = 30°$ direction, $f_{\text{co}}/f_{\text{peak}} \simeq 6.7$. Comparing the $r = 0.67$ and $r = 1.52$ cases, the SPL reductions are approximately equal, as a result of the balance between a gain of noise reduction near f_{peak} and a loss of noise reduction at frequencies greater than f_{co}.

The increase in high frequency noise may have two different origins: it could either result from the microjets system alone or originate in the interaction between the microjets and the mixing layer of the main jet. The first hypothesis has to be rejected by the analysis of the noise spectrum of microjets alone (not represented), because the noise level is always less than 10 dB with respect to the reference jet noise spectrum. Hence at high frequencies, above 10 kHz, the increase can only be due to a non-linear interaction between the microjet and the initial mixing layer of the jet.

5. Effect of the number of microjets

The results in this section are given for d set to zero, as in Section 4, and the jet Mach number is $M_j = 0.9$. The number of microjets was successively set to $n = \mathbf{3}$, **6**, **12**, **15** and **18** in an azimuthal periodic scheme. For example, **3** corresponds to 1 microjet operating every 6 microjet positions, and **15** corresponds to 5 consecutive microjets operating every 6 microjet positions. This study aims at determining the influence on jet noise reduction of an increasing number of microjets n. Results are given in Fig. 5 for two values of velocity ratios: $r = 0.32$ and $r = 1.10$. In Fig. 5, the total mass flux ratio, i.e., the ratio between the injected mass flux of the microjets system and the mass flux of the main jet, $r_m = \sum_{k=1}^{n} (\rho_k U_k S_k)/\rho_0 U_j S_j$.

First, we observe that a noise reduction of the order of 2 dB is obtained for a mass flux ratio below 0.005. As a comparison, for the water injection technique, the mass flux ratio necessary to achieve a reduction of 2 dB for a cold $M_j = 0.8$ jet is about 0.3 [12].

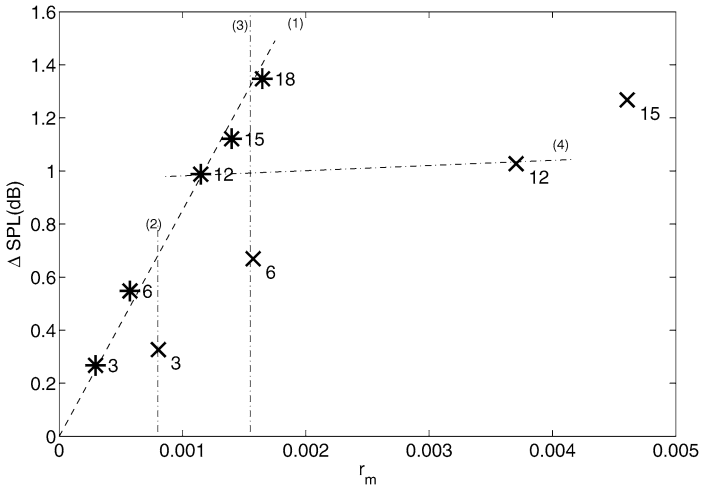

Fig. 5. Jet noise reduction at $\theta = 90°$, as a function of the total mass flux ratio r_m, for $r = 0.32$ (∗) and $r = 1.10$ (×). The number of microjets is indicated by the subscript near each point. $d = 0$ and $M_j = 0.9$.

Fig. 5. Réduction du bruit de jet à $\theta = 90°$ en fonction du rapport des débits massiques r_m, pour $r = 0{,}32$ (∗) et $r = 1{,}10$ (×). Le nombre de microjets utilisés est indiqué pour chaque point. $d = 0$ et $M_j = 0{,}9$.

The data in Fig. 5 can be examined either in considering the effect of varying n with a given microjet velocity or the effect of varying n with a given total mass flux ratio.

For a given microjet velocity, one observes a linear dependency of the noise reduction with the number of microjets. The line (1) on Fig. 5 highlights this trend for $r = 0.32$. Consequently, it seems that this control acts without implying any azimuthal modal response of the jet, and that it is simply proportional to the area of the mixing layer impacted by microjets.

For a given total mass flux ratio, the maximum noise reduction is obtained for the configuration with the highest number of microjets (see Fig. 5, lines (2) and (3)), i.e., the one with the lowest microjets velocity. This confirms the crucial role of n, which appears to be more decisive for noise reduction than the microjet velocity. Indeed, as illustrated by line (4), an increase of r from $r = 0.32$ to $r = 1.10$ does not modify significantly the noise reduction, as previously explained by the noise spectra evolution in Section 4.

6. Conclusion

A microjets system has been developed to reduce the noise emitted by high speed jets. The typical noise reduction is about 2 dB for a jet with a Mach number $M_j = 0.7$, when the mass flux in the microjets system is of order 0.003 of the main jet mass flux. A parametric study has shown how the noise reduction is affected by the microjet velocity relative to the main jet velocity, the longitudinal distance between the point of injection and the nozzle exit, and by the number of microjets. The maximum noise reduction in our experiments was obtained with a microjets system which:

- is applied close to the jet exit, to act on a sensitive mixing layer;
- maximizes the number of microjets n, knowing that a proportional relation between this parameter and the noise reduction was obtained in the scope of this study. By increasing n, the interaction zone between the microjets and the main jet is increased;
- implies a microjet velocity as high as possible, the upper limit being given by the interaction noise level causing noise regeneration. A balance has to be found between noise reduction, interaction noise in high frequencies and total mass flux injected.

The aerodynamical part of this aeroacoustical study is currently being addressed, notably in order to determine the modification of the turbulent field linked with noise reduction. A PIV study in successive planes perpendicular to the axis of a $M_j = 0.1$ jet indicates a strong modification of the longitudinal vorticity field. This could be responsible for the reduction of the turbulent mean velocity, as it has been demonstrated in other cases of fluidic control [13]. A pair of longitudinal counter-rotating vortices is generated by each microjet, and the dependency of jet noise reduction with the number of microjets n could result from a local reduction of the turbulence level by these pairs of vortices.

References

[1] C.K.W. Tam, Jet noise generated by large-scale coherent motion, in: H.H. Hubbard (Ed.), Aeroacoustics of Flight Vehicles, vol. 1, Noise Sources, 1995, pp. 311–390.
[2] R. Westley, G.M. Lilley, An investigation of the noise field from a small jet and methods for its reduction, College of Aeronautics Cranfield Report, N° 53, 1952.
[3] J.C. Simonich, S. Narayanan, Aeroacoustic characterization, noise reduction and dimensional scaling effects of high subsonic jets, AIAA J. 39 (11) (2001) 2062–2069.
[4] K.M.B.Q. Zaman, Effects of delta tabs on mixing and axis switching in jets from axisymmetric nozzles, AIAA Paper 94-0186, 1994.
[5] K.M.B.Q. Zaman, Spreading characteristics of compressible jets from nozzles of various geometries, J. Fluid. Mech. 383 (1999) 197–228.
[6] V.H. Arakeri, A. Krothapalli, On the use of microjets to suppress turbulence in a Mach 0.9 axisymmetric jet, J. Fluid. Mech. 490 (2003) 75–98.
[7] S. Lewy, Acoustique industrielle et aéroacoustique, Hermes, 2000.
[8] T. Castelain, M. Dietrich, J.C. Béra, M. Sunyach, Contrôle par microjets d'une couche de mélange: exploitation de mesures PIV synchronisées, in: 40ème Colloque d'Aérodynamique Appliquée, Toulouse, France, mars 2005.
[9] A.K.M.F. Hussain, M.A.Z. Hasan, Turbulence suppression in free turbulent shear flows under controlled excitation. Part 2: Jet-noise reduction, J. Fluid. Mech. 150 (1985) 159–168.
[10] C.K.W. Tam, Jet noise since 1952, Theor. Comput. Fluid Dyn. 10 (1998) 393–405.
[11] K.M.B.Q. Zaman, J.C. Yu, Power spectral density of subsonic jet noise, J. Sound Vib. 98 (1985) 519–537.
[12] T. Norum, Reductions in multi-component jet noise by water injection, in: 10th AIAA/CEAS Aeroacoutics Conference, Manchester, United Kingdom, AIAA-2004-2976, 2004, http://hdl.handle.net/2002/15630.
[13] G.M. Di Cicca, G. Iuso, P.G. Spazzini, M. Onorato, PIV study of the influence of large-scale streamwise vortices on a turbulent boundary layer, Exp. Fluids 33 (2002) 663–669.